Self-Assembly

DOI: 10.1002/anie.200903658

Hollow Six-Stranded Helical Columns of a Helicene**

Maxim A. Shcherbina, Xiang-bing Zeng, Timur Tadjiev, Goran Ungar, S. H. Eichhorn, Karen E. S. Phillips, and Thomas J. Katz*

Much studied have been the helical columnar liquid-crystalline phases of many materials, including such lyotropic systems as the polymers DNA, poly(γ-benzyl-L-glutamate), and xanthan[1] and such thermotropic materials, some with chiral side chains,[2] as triphenylenes,[3] banana-shaped molecules,[4] mesomorphic twin molecules,[5] foldamers,[6] wedge-shaped molecules (including dendrons, either free or attached to polymer backbones),[7–9] crown ethers,[10] polyphenylacetylenes,[11] and star-shaped molecules.[12–14] But the columnar liquid-crystalline phases of helicenes[15,16] have been studied very little, even though they are particularly interesting because the cores of their constituent molecules are chiral.

Herein we analyze by means of X-ray scattering, in conjunction with electron-density reconstruction, molecular dynamics, and scattering pattern simulation, the supermolecular structures of the materials formed when molecules of one such helicene (**1** in Figure 1 a), both racemic and enantiopure, assemble in well-aligned fibers. The enantiopure material, synthesized previously,[16a] was shown to exhibit strong circularly polarized fluorescence[16a] and strong second harmonic generation.[16b] Like a related structure,[17] it was thought to be comprised of molecules that stack on one another as in discotic phases. Instead, it is shown herein that the molecules assemble into hexagonal phases comprised of hollow-centered 13_2 helical columns, illustrated in Figure 1 and Figure 3.

Both racemic and enantiopure **1** are ductile (plastic) solids that melt into isotropic liquids at 215 °C (40 kJ mol^{-1}) and 242 °C (47 kJ mol^{-1}), respectively. No other transitions are observed by polarized light microscopy, differential scanning calorimetry (DSC), and X-ray diffraction. Thermal gravimetric measurements confirm that both compounds under nitrogen are chemically stable up to 285 °C, but DSC heating and cooling experiments show that enantiomerically pure **1** slowly racemizes upon melting into the isotropic phase.

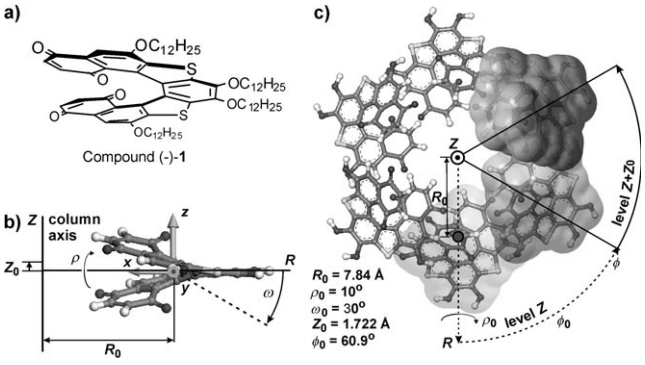

Figure 1. a) Compound (−)-**1**. b) The definition of coordinates. *x*,*y*,*z* are principal axes of the molecular mass tensor. *Z*, *R*, ϕ are cylindrical coordinates with the column axis as reference (note that the $OC_{12}H_{25}$ groups are replaced by OH groups in the derivation of the tensor). Adjustable parameters: R_0 is the distance of the molecular center of mass from the column axis; ω_0 is the molecular tilt, that is, rotation around *y*; ρ_0 is the "propeller blade" rotation around *R*. c) Arrangement of the heterohelicenes in the six-molecule asymmetric unit: molecule $i+1$ is related to molecule i by rotation around *Z* by ϕ_0 and translation along *Z* by Z_0. The best-fit parameters are listed.

Fibers were drawn from 10 wt % solutions in heptane at 80 °C and investigated by wide-angle (WAXS) and small-angle (SAXS) diffraction of synchrotron-generated X-rays.[18] Figure 2 a,c shows the WAXS and SAXS patterns of the racemic fiber. The pattern of enantiopure (−)-**1** is indistinguishable from that of *rac*-**1**, except for the position of the small-angle reflection marked by the arrow in Figure 2 c,d. Additional still wider angle diffraction patters show no sharp reflections in the $2\pi/q$ region of 0.3–0.5 nm, thus confirming the liquid-crystallinity of **1**.

The experimental fiber X-ray patterns show sharp Bragg reflections on layer lines 0 and 2 and diffuse streaks on the others. The equatorial reflections, with q^2 values in the ratio 1:3:4:7:9:12:13 (see Table S1 in the Supporting Information) typify hexagonal order. The indexing in Figure 2 c is in terms of *h* and *k* for a 2D hexagonal lattice. The cell parameter $a_{hex} = 4.001$ nm. The diffuse streaks on the higher layer lines form a triple cross pattern, with the centers of the first, second, and third meridional crosses on the 0, 13, and 26 layer lines. Near the 0th and 26th layers only even lines are observed, namely, the 0th, 2nd, 4th, and 24th (weak), 26th, 28th, and 30th (weak). In contrast, near the 13th layer

[*] Dr. M. A. Shcherbina, Dr. X.-b. Zeng, T. Tadjiev, Prof. G. Ungar
Department of Engineering Materials, University of Sheffield
Sheffield, S1 3JD (UK)
E-mail: g.ungar@sheffield.ac.uk
Prof. S. H. Eichhorn
Department of Chemistry and Biochemistry, University of Windsor
Windsor ON, N9B 3P4 (Canada)
Prof. K. E. S. Phillips
Department of Chemistry, Hunter College of CUNY
695 Park Avenue, New York, NY 10065 (USA)
Prof. T. J. Katz
Department of Chemistry, Columbia University
3000 Broadway, New York, NY 10027 (USA)

[**] G.U. acknowledges the financial support from EPSRC and the ESF Eurocores SONS2 project SCALES. S.H.E. thanks NSERC and CFI/OIT for financial support. We thank Drs. G. Grossmann and N. Terrill for their help in setting up the experiments at Daresbury and Diamond, and Prof. S. Z. D. Cheng of Akron University for density measurements.

Supporting information for this article is available on the WWW under http://dx.doi.org/10.1002/anie.200903658.

© 2009 Wiley-VCH Verlag GmbH & Co. KGaA, Weinheim

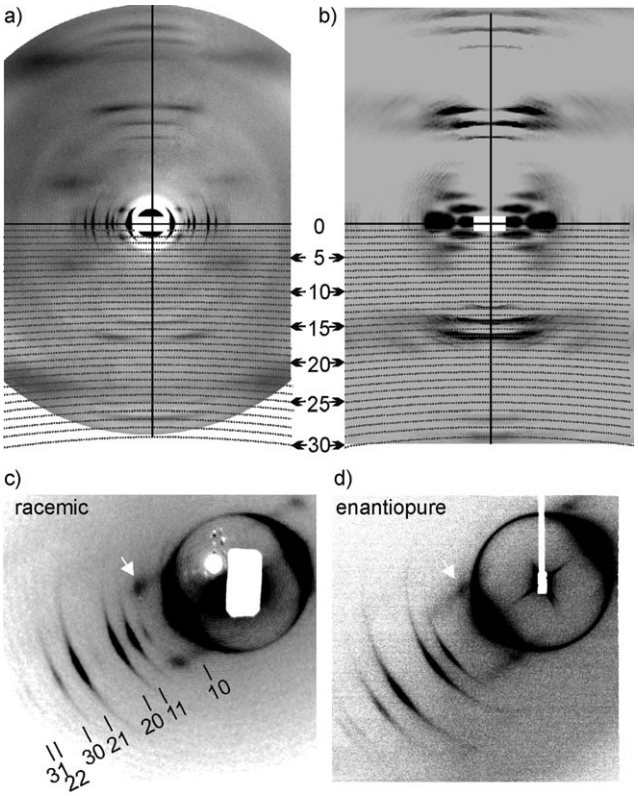

Figure 2. a) Experimental and b) simulated WAXS and c,d) experimental SAXS fiber patterns of **1**. a,c) *rac*-**1**, d) (−)-**1**. The fiber axis is vertical in (a,b) and tilted in (c,d). Part (b) shows the simulated single-column diffraction pattern of the best-fit structure shown in Figure 1c and Figure 3. Numbered layer lines are superimposed on the bottom half of (a) and (b). The strong diffuse scatter on the 0th and 2nd layer lines in the diffraction pattern of an isolated column in (b) condenses into a series of sharp Bragg reflections in (a) owing to the long-range order in column positions.

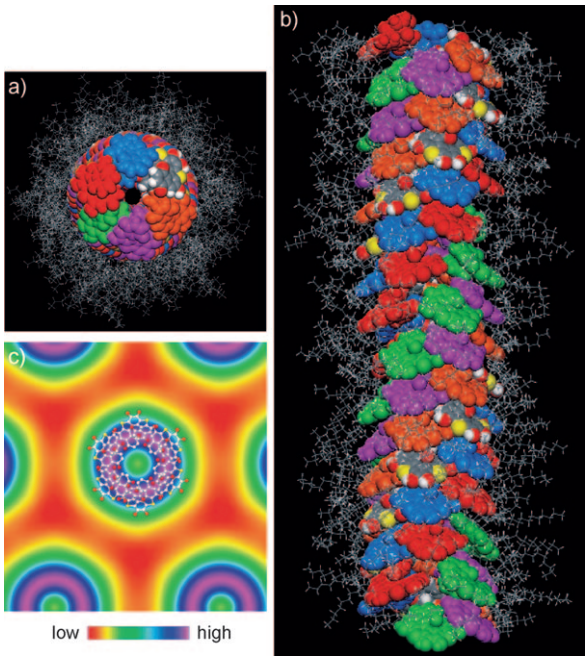

Figure 3. Molecular organization in the six-stranded 13_2 helical column of (−)-**1**. a,c) Views along column axis, b) side view. In (a), the aromatic cores and the alkyl tails are shown with space-filling and stick models, respectively, while in (c) only the aromatic cores of one six-molecule asymmetric unit are shown as ball-and-stick. In (c) an asymmetric unit, without hydrogen atoms, is superimposed on the electron density map, illustrating the origin of the high-electron-density ring (purple). See also Figure S1.

scattering is visible only on odd lines: the 11th (weak), 13th, 15th, and 17th. Such a pattern characterizes a 13_2 helix.[19] Thus the structure consists of 13_2 helical columns sited on a hexagonal 2D lattice, with long-range order in the XY plane. The helices on neighboring columns are only weakly correlated (see below). The layer-line spacing, $d_{layer} = 11.19$ nm, equals c_0, the repeat period along the column axis. But the pitch of the continuous helix, that is, of the helical column disregarding its internal structure, is $c_0/2 = 5.56$ nm.

Had the helicene molecules, like those in most discotic liquid crystals, stacked on top of one another as previously suggested,[16] there would have been 13 molecules in a unit cell. The corresponding density, given the measured cell dimensions, would have been only 0.16 g cm^{-3}. However, the experimentally measured density is 1.058 ± 0.002 g cm^{-3} at 20 °C, more than six times higher. This result means that a helical repeat unit consists of six or seven helicene molecules, not just one. Moreover, while Figure 3c exhibits the expected circular high electron density (ED) zone representing the aromatic core of each column, it also shows in the very center a fairly deep ED minimum, indicative of a void in the center of the column (for ED determination, see the Supporting Information). We note that a similar central void was reported recently in the columns of some taper-shaped benzyl ether based dendrons.[20]

To find out how the molecules assemble, attempts were made to build a reasonably close-packed motif of six to seven molecules, which led naturally to a ring of six or seven tilted molecules arranged in a truncated cone (see Figure 1c, Figure 3a, and Figure S1 in the Supporting Information for six molecules). By rotating the molecules around two axes, x and y, six molecules could be fitted around the ring with a high packing efficiency, while with seven molecules steric clashes could not be avoided. These models were subjected to constant pressure annealing dynamics simulations and energy minimizations (Forcite Plus, Universal force field[21]) to try, in the first instance, to find a similarity between the structure projected onto the XY plane and the ED map.

For a more systematic structure refinement, internal molecular coordinate axes x,y,z (see Figure 1b) were obtained by diagonalizing the molecular mass tensor. A single 13_2 helical column was then built from such six-molecule motifs, with the dodecyloxy chains replaced by methoxy groups. Fibrehelix[22] was used at this stage to simulate the diffraction pattern. Five parameters had to be adjusted (Figure 1b,c): R_0, the distance of the molecular center of gravity from the column axis; ρ_0, the angle of rotation around the radius R; ω_0, the tilt around the internal coordinate axis y; and ϕ_0 and Z_0, the rotation around and the shift along the Z axis between successive molecules. R_0 was determined from the equatorial ED map in Figure 3c. Z_0 was

 © 2009 Wiley-VCH Verlag GmbH & Co. KGaA, Weinheim

initially set at $c/(13\times6)$. ρ_0, ω_0, ϕ_0, and Z_0 were then varied, and the optimum values for ϕ_0 and Z_0, as well as the range for ϕ_0 and ω_0, were chosen on the basis of diffraction patterns simulated first by Fibrehelix and subsequently and more realistically by Cerius-2.[21] Dynamically disordered dodecyl chains were added, and the structure was refined by varying ρ_0 and ω_0, (for details see the Supporting Information). The match between the measured and calculated layer-line intensity distributions is shown in Table S2 in the Supporting Information. The best values for all the structural parameters are displayed in Figure 1.

The best simulated WAXS fiber pattern is shown in Figure 2b, which should be compared with Figure 2a. Figure 3b shows the side view of just over one repeat along the column axis. One full repeat of (−)-**1** contains two turns of a right-handed helix and 13 motifs of six molecules each, that is, 65 molecules total. The structure can be considered a six-stranded 13_2 helix, since in Figure 3b a helicoidal line connects molecules of the same color for each of the six helicenes comprising an asymmetric unit. The arrangement of the six (−)-**1** molecules within the asymmetric unit is close to a right-handed helix, that is, both ϕ_0 and Z_0 are positive.

Since the columns in the simulated pattern are not on a lattice, the scattering on all layer lines with $l>2$ is diffuse. Heterohelicene **1** has an awkward shape for stacking in columns; hence the unusual self-assembly mode. However, the "pine-tree" structure based on tilted ($\rho_0>0$) phenyl rings has previously been found in columns formed by less awkwardly shaped benzyl ether based mesogens.[7] For the four dodecyl chains to stay at the column periphery, the thick region of the molecule, where the quinone rings overlap, must be near the column's center. The relatively high tilt ρ_0 in combination with a suitable ϕ_0 enables the thick quinone parts of the molecules to stagger. It would appear that the very diffuse off-meridional scatter, observed between layer lines 21 and 24 and not reproduced by the simulation in Figure 2b, may be due to the partially ordered alkyl chains somewhat tilted away from the equatorial plane.

The nonzero layer lines consist of diffuse streaks, indicating that the internal structures of different columns are uncorrelated. But the equatorial reflections are radially sharp and resolution-limited, showing that there is true long-range order among column positions on the 2D hexagonal lattice. The structure is thus that of a liquid crystal. Of special interest is the relatively sharp reflection on the 2nd layer line, marked with white arrows in Figure 2c,d. This is the only diffraction feature that distinguishes enantiopure **1** from racemic **1**. In the former (Figure 2d), the reflection can be indexed as (102). However, in the racemate this reflection is shifted along the layer line further away from the meridian and is incommensurate with the hexagonal lattice. Its existence indicates that there is a degree of long-range correlation between the helices in longitudinal position and angle of rotation around the helix axis. However, that no other sharp non-equatorial reflections are seen means that these correlations are weak and that the mean square deviation is high. Significantly, the correlation is between helical envelopes rather than the individual molecules. While an ideal 3D hexagonal structure consisting of static helices of the same hand allows all helices to have the same position and rotation angle (the situation approached by enantiopure (−)-**1**, see Figure 4a,c), hexagonal symmetry must be broken if half the helices are right- and half left-handed, as envisaged for *rac*-**1** in Figure 4b,d. Generally, in ordered 1:1 mixtures of right- and left-handed helices, the symmetry is reduced to triclinic, but monoclinic or orthorhombic are possible for discrete helices, as, for example, in the α-form of isotactic polypropylene.[23] The symmetry of *rac*-**1** cannot be established just from one non-equatorial reflection, but it is clear that, while the reciprocal X^*Y^* plane is perpendicular to the fiber axis, Z^* is tilted. Hence the helices are still parallel to the fiber but are sheared longitudinally (Figure 4d). In fact, Figure 2c,d shows a weak streak along the 2nd layer line in addition to the Bragg reflection, indicative of shear defects.

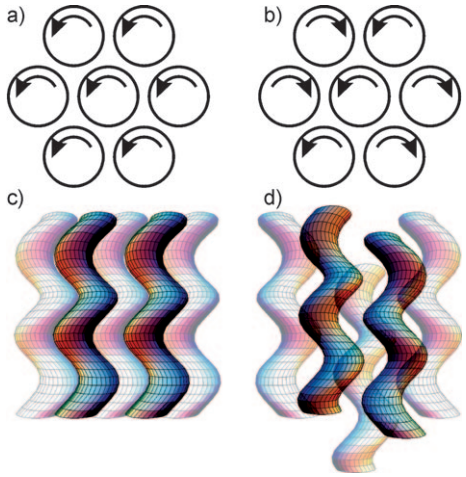

Figure 4. Stacking of helical columns (schematic). a, c) enantiopure compound, b, d) racemate, with enantiomers segregated in separate right and left helical columns. In the top view (a,b) arrows show the sense of the helix. In (c,d) the darker helices are in the front row, the pale helices are behind. The helical amplitude is grossly exaggerated.

The spontaneous resolution of (−)-**1** and (+)-**1** enantiomers into, respectively, right- and left-handed helical columns forming an ordered array, is an unusual mesoscale racemate, not a crystalline racemate, but not a conglomerate either.

The work herein shows that enantiopure and racemic helicenebisquinones **1** form hexagonal columnar phases in which the internal structures of the columns are 13_2 hollow helices comprised of six-molecule repeat units, hence of 78 molecules and two turns in an 11.2 nm period. The long-range order among the columns is laterally high and longitudinally low. Enantiomer (−)-**1** forms a true hexagonal structure of right-handed helices; columns of segregated enantiomers in *rac*-**1** are displaced longitudinally. For the alkoxy substituents to face outward, the unsubstituted quinones face inward. Because the helicenes cannot tesselate like wedge-shaped molecules,[24] they leave a void in the column center. These results point to a route to chiral porous materials.

Received: July 4, 2009
Published online: September 8, 2009

 © 2009 Wiley-VCH Verlag GmbH & Co. KGaA, Weinheim

Keywords: chirality · columnar phases · liquid crystals · racemic mixtures · X-ray diffraction

[1] a) F. Livolant, Y. Bouligand, *J. Phys.* **1986**, *47*, 1813 – 1827; b) M. Nakata, G. Zanchetta, B. D. Chapman, C. D. Jones, J. O. Cross, R. Pindak, T. Bellini, N. A. Clark, *Science* **2007**, *318*, 1276 – 1279.

[2] J. Malthête, J. Jacques, N.-H. Tinh, C. Destrade, *Nature* **1982**, *298*, 46 – 48.

[3] a) E. F. Gramsbergen, H. J. Hoving, W. H. de Jeu, K. Praefcke, B. Kohne, *Liq. Cryst.* **1986**, *1*, 397 – 400; b) E. Fontes, P. Heiney, W. H. de Jeu, *Phys. Rev. Lett.* **1988**, *61*, 1202 – 1205; c) A. N. Cammidge, H. Gopee, *J. Mater. Chem.* **2001**, *11*, 2773 – 2783; d) S. Ishihara, Y. Furuki, S. Takeoka, *Polym. Adv. Technol.* **2008**, *19*, 1097 – 1104.

[4] a) H. R. Brand, P. E. Cladis, H. Pleiner, *Europhys. Lett.* **2002**, *57*, 368; b) Yu. A. Nastishin, M. F. Achard, H. T. Nguyen, M. Kleman, *Eur. Phys. J. E* **2003**, *12*, 581 – 591.

[5] D. Goldmann, S. Mahlstedt, D. Janietz, P. Busch, C. Schmidt, A. Stracke, J. H. Wendorff, *Liq. Cryst.* **1998**, *24*, 881 – 890.

[6] a) S. H. Gellman, *Acc. Chem. Res.* **1998**, *31*, 173 – 180; b) S. Hecht, I. Huc, *Foldamers: Structure, Properties and Applications*, Wiley-VCH, Weinheim, **2007**; c) R. A. Smaldone, J. S. Moore, *Chem. Eur. J.* **2008**, *14*, 2650 – 2657.

[7] a) Y.-K. Kwon, C. Danko, S. N. Chvalun, J. Blackwell, V. Percec, J. A. Heck, *Macromol. Symp.* **1994**, *87*, 103; b) Y.-K. Kwon, S. N. Chvalun, A.-I. Schneider, J. Blackwell, V. Percec, J. A. Heck, *Macromolecules* **1994**, *27*, 6129 – 6132; c) Y.-K. Kwon, S. N. Chvalun, J. Blackwell, V. Percec, J. A. Heck, *Macromolecules* **1995**, *28*, 1552 – 1558; d) S. N. Chvalun, M. A. Shcherbina, I. V. Bykova, J. Blackwell, V. Percec, *J. Polym. Sci. Part A* **2002**, *45*, 1281 – 1289.

[8] V. Percec, M. Glodde, T. K. Bera, Y. Miura, I. Shiyanovskaya, K. D. Singer, V. S. K. Balagurusamy, P. A. Heiney, I. Schnell, A. Rapp, H. W. Spiess, S. D. Hudson, H. Duan, *Nature* **2002**, *417*, 384 – 388.

[9] a) V. Percec, B. C. Won, M. Peterca, P. A. Heiney, *J. Am. Chem. Soc.* **2007**, *129*, 11265 – 11278; b) V. Percec, J. G. Rudick, M. Peterca, P. A. Heiney, *J. Am. Chem. Soc.* **2008**, *130*, 7503 – 7508.

[10] A. M. Levelut, J. Malthete, A. Collet, *J. Phys.* **1986**, *47*, 351 – 357.

[11] K. Huang, M. Tabata, Y. Mawatari, A. Miyasaka, E. Sato, Y. Sadahiro, Y. Kashiwaya, K. Ishii, *J. Polym. Sci. Part A Polym. Chem.* **2005**, *43*, 2836 – 2850.

[12] J. Barberá, J. Jimenez, A. Laguna, L. Oriol, S. Perez, J. L. Serrano, *Chem. Mater.* **2006**, *18*, 5437 – 5445.

[13] Z. Tomovic, J. van Dongen, S. G. George, H. Xu, W. Pisula, P. Leclere, M. M. J. Smulders, S. De Feyter, E. W. Meijer, A. P. H. J. Schenning, *J. Am. Chem. Soc.* **2007**, *129*, 16190 – 16196.

[14] J. Wu, W. Pisula, K. Mullen, *Chem. Rev.* **2007**, *107*, 718 – 747.

[15] C. Nuckolls, T. J. Katz, *J. Am. Chem. Soc.* **1998**, *120*, 9541 – 9544.

[16] a) K. E. S. Phillips, T. J. Katz, S. Jockusch, A. J. Lovinger, N. J. Turro, *J. Am. Chem. Soc.* **2001**, *123*, 11899 – 11907; b) T. Verbiest, S. Van Elshocht, A. Persoons, C. Nuckolls, K. E. S. Phillips, T. J. Katz, *Langmuir* **2001**, *17*, 4685 – 4687; c) L. Vyklický, S. E. Eichhorn, T. J. Katz, *Chem. Mater.* **2003**, *15*, 3594 – 3601.

[17] a) C. Nuckolls, T. J. Katz, G. Katz, P. J. Collings, L. Castellanos, *J. Am. Chem. Soc.* **1999**, *121*, 79, and references therein; b) References cited in reference [16a].

[18] Herein, WAXS and SAXS refer, respectively, to $q \leq 18$ and $q \leq 5.2\ \mathrm{nm}^{-1}$ ($q = [4\pi \sin\theta]/\lambda$, θ = scattering half angle, λ = X-ray wavelength), or $d = 2\pi/q \geq 0.36$ and $d \geq 0.12$ nm.

[19] a) W. Cochran, F. H. C. Crick, V. Vand, *Acta Crystallogr.* **1952**, *5*, 581 – 586; b) R. E. Franklin, A. Klug, *Acta Crystallogr.* **1955**, *8*, 777 – 780.

[20] V. Percec, A. E. Dulcey, V. S. K. Balagurusamy, Y. Miura, J. Smidrkal, M. Peterca, S. Nummelin, U. Edlund, S. D. Hudson, P. A. Heiney, D. A. Hu, S. N. Magonov, S. A. Vinogradov, *Nature* **2004**, *430*, 764 – 768.

[21] Materials Studio 4.0 from Accelrys, Inc., module ForcitePlus, using Universal Force Field (A. K. Rappé, C. J. Casewit, K. S. Colwell, W. A. Goddard, W. M. Skiff, *J. Am. Chem. Soc.* **1992**, *114*, 10024 – 10035).

[22] D. Dominguez-Sal, X. Messeguera, J. A. Subirana, *Acta Crystallogr. Sect. D* **2004**, *61i*, 203 – 206.

[23] G. Natta, P. Pino, P. Corradini, *J. Am. Chem. Soc.* **1955**, *77*, 1708 – 1710.

[24] V. Percec, J. Heck, G. Johansson, D. Tomazos, M. Kawasumi, G. Ungar, *J. Macromol. Sci. Part A* **1994**, *31*, 1031 – 1070; V. Percec, M. N. Holerca, S. Uchida, W. D. Cho, G. Ungar, Y. S. Lee, D. J.P Yeardley, *Chem. Eur. J.* **2002**, *8*, 1106 – 1117.

 © 2009 Wiley-VCH Verlag GmbH & Co. KGaA, Weinheim